Influence of Rotor Pole Arc on the Flux-Weakening Range of a Doubly Salient Switched Reluctance Motor

Hedi Yahia, Rachid Dhifaoui, Bernard Multon

CESA '98

INFLUENCE OF ROTOR POLE ARC ON THE SPEED RANGE IN FLUX-WEAKENING MODE OF A DOUBLY-SALIENT SWITCHED RELUCTANCE MOTOR

H. YAHIA, R. DHIFAOUI
Ecole Nationale d'Ingénieurs de Monastir, 5000 Monastir - Tunisia
B. MULTON
Ecole Normale Supérieure de Cachan (LESiR), 61 Av. du P^{dt} Wilson - France

Keywords: Flux-Weakening, SRM, Rotor Pole Arc, Constant Maximal Power, Constant Maximal Torque, Torque Ripple.

ABSTRACT

In the present work we studied the possibilities of operating Switched Reluctance Motor (SRM) in regime of flux-weakening. The influence of control and geometrical parameters has been investigated and is presented for a 4 kW machine of the type OULTON™ 8/6. We studied especially the effect of the rotor pole arc (β_r°) on the zone of flux-weakening. A purpose-built rotor with a different β_r° fabricated in a framework of collaboration with two Tunisian companies has allowed validation of the numerical results.

1. INTRODUCTION

The number always growing of studies devoted to the Switched Reluctance Motor (SRM) shows the interest of manufacturers and academics alike in this type of machines. The SRM presents intrinsically undeniable advantages in terms of fabrication cost and robustness thanks to its simple and perfectly balanced rotor structure. These machines are well suited to applications where strong torque-low speed (e.g., traction, robotics) or strong power-high speed (e.g., machine tools, electrical vehicles) combinations are required. Thus they rival their synchronous and "brushless" counterparts [1].

The influence of dimensional parameters is examined in this paper using a purpose-built rotor fabricated using hot-rolled sheet of the type M5-30 3/10^e [2]. The tooth angle of the rotor (β_r°) has a direct influence on the constraints: torque ripple at low speed and operating range at constant maximal power. The average torque is dependant on β_r° and increases with decreasing β_r° for all modes of operation.

2. TORQUE/SPEED CHARACTERISTICS

Torque/speed characteristics of the SRM are not defined only by geometrical parameters. Indeed it is possible, thanks to adequate control to modify trends of these characteristics. In general, the torque/speed characteristics envelope of such a SRM is given by Figure 1.

These characteristics resemble those of continuous current electric motors operated with separated excitation. The control of the supply current and the terminal voltage is achieved by Pulse With Modulation (PWM). Additionally, varying switching angle and using appropriate strategies enable a wide range of different characteristics to be obtained [3].

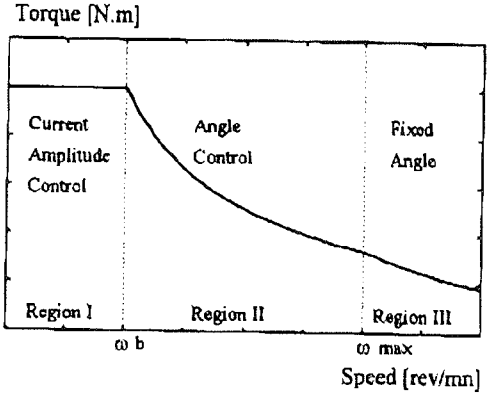

Figure 1: Torque/Speed characteristics of a SRM

3. SIZE PARAMETERS

Figure 2 gives the main dimensions of the 4 kW OULTON™ motor used. It has an 8/6 structure (stator with 8 teeth and 4 phases, rotor with 6 teeth).

The main geometrical parameters associated with the SRM structure are:

N_r:	number of the rotor teeth = 6
N_s:	number of the stator teeth = 8
e:	width of air gap = 0.3 mm
e_c:	thickness of the yoke = 10.5 mm
h_r:	height of rotor teeth = 17.6 mm
h_s:	height of stator teeth = 30.4 mm
r:	radius of the rotor = 47.8 mm
β_r°:	rotor pole arc = 21°
β_s°:	stator pole arc = 20°
n:	number of turns per phase = 186

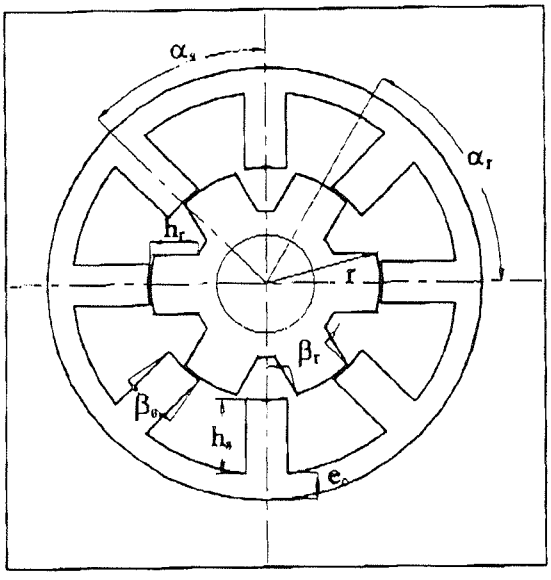

Figure 2: Dimensional parameters of the OULTON™ machine used

Among the numerous fundamental conditions defining an SRM structure, we are interested in those concerning poles angles (teeth). Indeed, to be able to start the machine when loaded independently of the position, it is necessary to produce a sufficient torque by feeding a single phase [4]. This is possible only if the electrical angle variation of the inductance ($D\theta_p$) defined by:

$D\theta_p = N_r \, Min(\beta_s°, \beta_r°)$ is greater than $\frac{2\pi}{q}$.

In the opposite case ($\beta_s° + \beta_r° > \frac{2\pi}{N_r}$), during powering of a given phase, we have superposition of negative and positive torque which cancel each other out. In order to ensure starting the machine, the following conditions must be fulfilled:

$$\beta_s^o + \beta_r^o > \frac{2\pi}{N_r} \quad (1)$$

or

$$\frac{N_r}{N_s}\beta_s + \beta_r < 1 \quad (2)$$

If $\beta_s^o > \beta_r^o$ and $\beta_{r\min} = \frac{1}{q}$ (3)

Then $\beta_{s\max} = \frac{N_s}{qN_r}(q-1)$ (4)

If $\beta_r^o > \beta_s^o$ and $\beta_{s\min} = \frac{N_s}{qN_r}$ (5)

then $\beta_{r\max} = 1 - \frac{1}{q}$ (6)

The constraints on pole arcs can be expressed graphically as in figure 3, in which the "feasible triangles" define the range of combinations normally permissible [5].

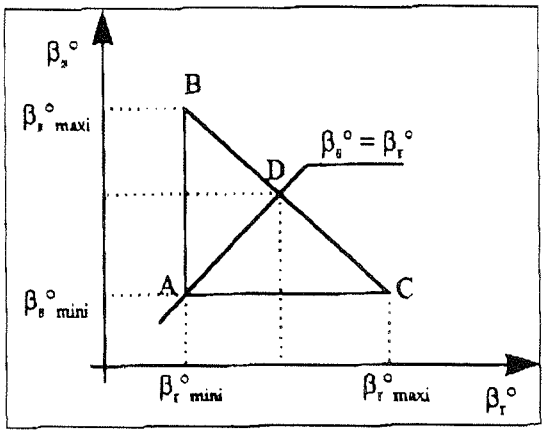

Figure 3: Pole-arc constraints – "feasible triangles"

The optimization of these parameters necessitates theoretical models of the machine in order to predetermine its electromagnetic characteristics. These information will be provided either by the waveform of linear permeance or by the set of flux characteristics (Φ (θ, i)) in saturated regime [6].

4. LINEAR MODELS

In a first approximation and for a given phase, the inductance L (θ) evolves linearly with the angle of overlapping of rotor and stator teeth [6]. It takes a minimal value (L_u) in unaligned and a maximal value (L_a) in aligned position. Between these two extreme values, we assume that the function L(θ) remains constant at L_{min} in unaligned position as the stator and rotor pole are not overlapped; i.e. during a mechanical angle equal to:

$$\theta_{po} = (\frac{2\pi}{N_r} - \beta_r° - \beta_s°) \quad (7)$$

After that the inductance starts a linear increase with rotation, until the poles are fully overlapped during an electrical angle:

$$D\theta p = N_r Min(\beta_s, \beta_r) \quad (8)$$

Finally, the inductance again remains constant at L_{max}, through the region of complete overlap, therefore during an electrical angle:

$$\theta_{pc} = N_r |\beta_s - \beta_r| \quad (9)$$

The idealized form wave of the inductance associated to the OULTON™ machine is represented in figure 3. When the magnetic circuit is not saturated and that magnetic losses and effects of edge are negligible, one can calculate analytically the aligned inductance (L_a):

$$L_a = n^2 k_f \mu_0 \frac{\beta_s 2\pi r l}{2 \; e \; N_s} \quad (10)$$

where

k_f: coefficient of buckling of griddles (<1)

r: radius of the rotor

Calculations of field by finite elements finish to determine rapidly the unaligned inductance from two fundamental parameters that are the ratio of the height of rotor teeth by the interpolar width of rotor $((1-\beta_r)\frac{2\pi}{N_r}r)$ and the ratio of this same interpolar width by the width of a stator teeth $(\beta_s \frac{2\pi}{N_s}r)$ [7].

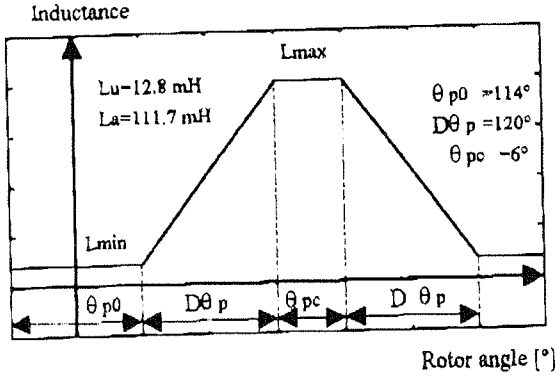

Figure 4: Spatial distribution of the inductance per phase of the OULTON™ machine

5. INFLUENCE OF CONTROL AND GEOMETRICAL PARAMETERS ON THE FLUX-WEAKENING RANGE

Feeding modes

Two feeding techniques are suited to the torque/speed characteristics of the SRM. The first mode is based upon the modulation of applied voltage. The second mode is based upon powering in full wave where the current and the torque are controlled by adjustment of angles of control θ_{on} and θ_{off}. In order reduce torque ripple and to fulfil some energy criteria, a torque control using square wave current is recommended [7]. Simulations have been done for a terminal voltage of 300V and a maximum current fixed at 15A. For speeds up to base speed (ω_b), the adopted mode of control is that in Trapezoidal Torque Waveform (TTW) (figure 5a). For higher speeds, the control in Full Wave Voltage (FWV) is used (figure 5b).

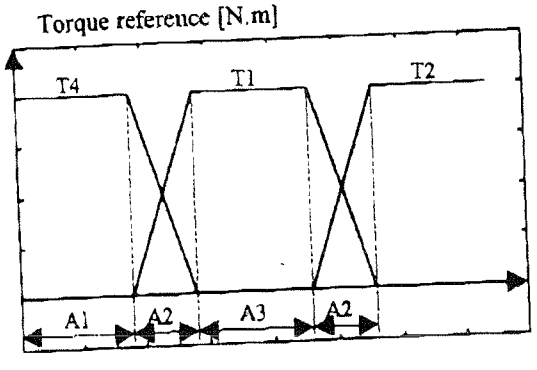

Figure 5a: Feeding of the SRM in trapezoidal wave form

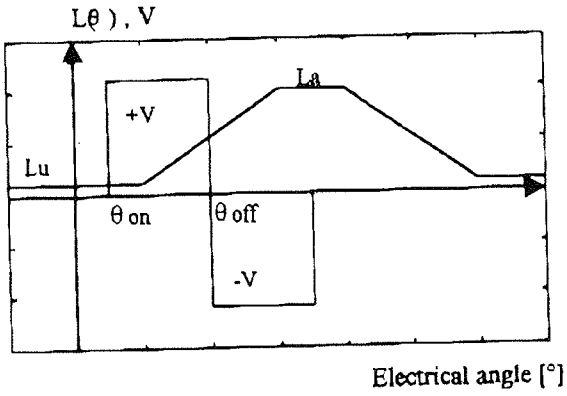

Figures 5b: Feeding of the SRM in the Full Wave Voltage

Influence of control parameters

From the spatial wave of the inductance, we defined numerically the two sets of characteristics $\Phi(\theta,i)$ and $T(\theta, i)$ in order to do more precise calculations of optimization from sets of characteristics collected numerically on the machine. For each calculated point determined by angles of torque A1 and A2 or by θ_{on} and θ_{off}, we have to know U_M, I_M, and I_{RMS} to be able to calculate the different optimization criteria. For all calculated points results are stocked to analyze the evolution of criteria of optimization as a function of working points.

The first results of simulation presented in figure 6 concern the limits of torque and convertible power ($<Tp>_{Max}.\Omega$) at given voltage and current in the presence the two modes of control. The power is normalized with respect to the nominal power of the machine (K_p=4000). The normalization of the torque is carried out with respect to that of the limit current of 15A (K_T=21). Figure 7 shows the evolution of parameters of control associated to the two modes that are respectively A1 and A2 for the torque control and θ_{on} and θ_{off} for the control in full wave voltage.

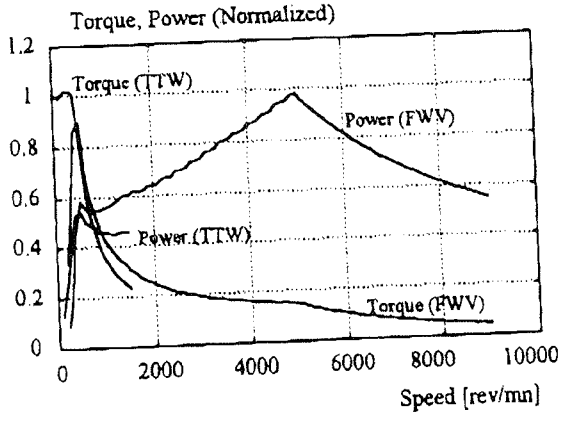

Figure 6: Torque and convertible Power

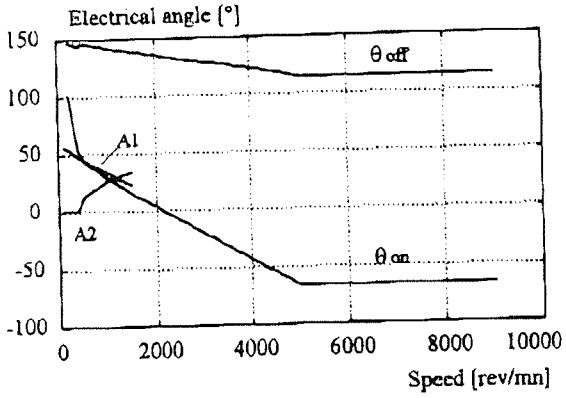

Figure 7: Evolution of angles of control at maximum power

As shown in Figure 6, we distinguish three classic regions of the torque/speed characteristics of a SRM. With the linear model associated to the OULTON™ machine, Table 1 provides the limits of these regions.

Regions	Region I	Region II	Region III
Mode of Operation	operation at maximum torque	operation at maximum power	natural characteristic
Range of speed	$0 < \Omega < 500$ rpm	$500 < \Omega <$ 5000 rpm	$\Omega > 5000$ rpm

Table 1: Limits of operation in linear regime

Influence of geometry parameters

For a given value of β_s (generally for starting and torque ripple considerations), the value of β_r is chosen according to constraints of moment of inertia and torque/speed characteristics obtained [8]. A high value of β_r gives a large aligned position that renders the flux weakening easier and allows a smoother torque by injection of appropriate waves of current. A low value of β_r gives an important unaligned position and allows the maximal power to increase ; however an instantaneous torque with small ripple becomes more difficult to obtain [9].

In order to study the sensitivity of the zone of operating at maximal power with respect to the rotor angle β_r for a given structure, two new rotors have been simulated with rotor mechanical angles of 30° and 12°. This choice corresponds to an increase and a decrease of 9° for β_r compared to β_r for the standard rotor. This choice enable us to cover the two parts of the triangle of feasibility. Only unaligned inductance (L_u) is affected by the variation of rotor angle β_r. The value of rotor pole arc has a considerable importance for the natural waveform of inductance or flux.

Analogous simulations (feeding modes and constraints, maximal voltage and RMS current) have been undertaken and their results are shown in figures 8 and 9 respectively for the two modes of control. The results already obtained with the standard rotor are also shown for comparison purposes. The effects of the variation of rotor pole arc of torque ripple are also shown respectively in figures 10 and 11, where the control angle optimizes the torque.

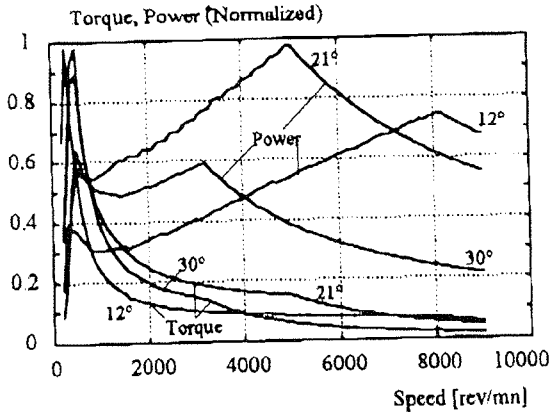

Figure 8: Influence of β_r on torque and power characteristics (control in full wave voltage)

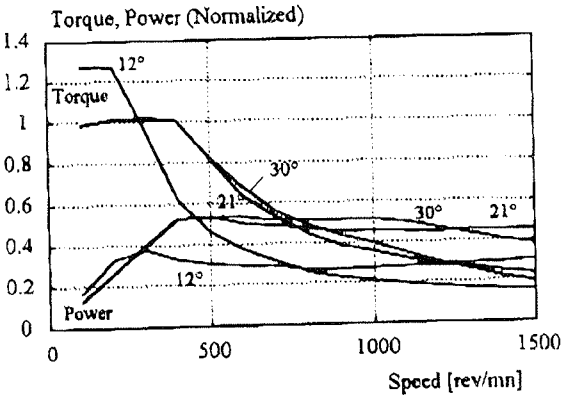

Figure 9: Influence of β_r on torque and power characteristics (control in trapezoidal torque waveform)

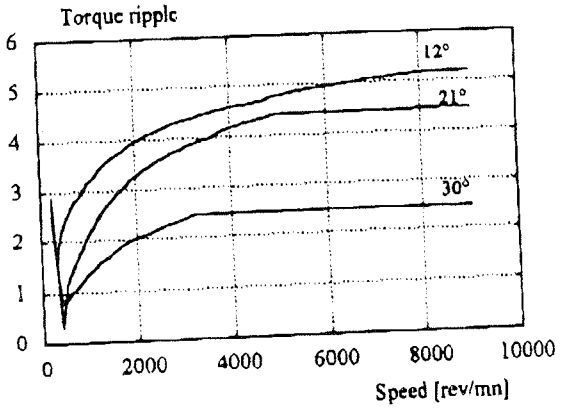

Figure 10: Influence of β_r on the torque ripple (control in full wave voltage)

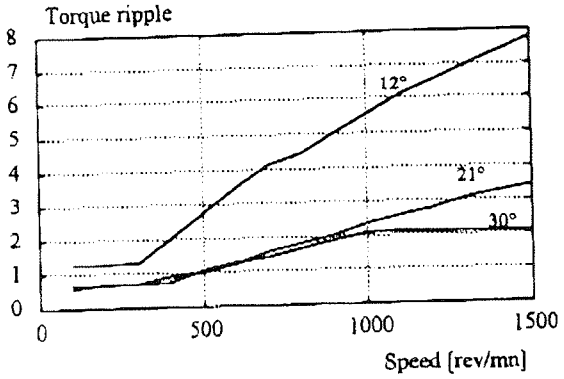

Figure 11: Influence of on the torque ripple (control in trapezoidal torque waveform)

With the two rotors having $\beta_r = 30°$ and 21°, respectively, we confirm the fact that the torque increases as β_r decreases. However, see $\beta_r = 12°$, we observed a lower torque value than that obtained with $\beta_r = 21°$. Thus, an optimal value of β_r must exist between the examined $\beta_r = 30°$ and $\beta_r = 12°$. This is the value of $\beta_r = 20°$ below which β_r should not decrease to attain the maximal torque.

With these two sets of characteristics, we have shown the effect of rotor pole arc on the maximization of the range of operation and on the torque ripple at maximum torque and power. This study based on linear models has enabled us to establish principles relative to all switched reluctance machines with large teeth. In the following we try to apply these principles to real prototypes.

Electromagnetic real models

The first used prototype is the 4 kW OULTON™ machine (8/6). Its real model is defined by the two characteristics $\Phi(\theta,i)$ and $T(\theta, i)$ determined experimentally [10]. The effect of stator pole arc is studied by the construction of a second rotor with a β_r of 30° and the corresponding real model is determined numerically.

The same simulation programs are used and the results are given in figures 12 and 13.

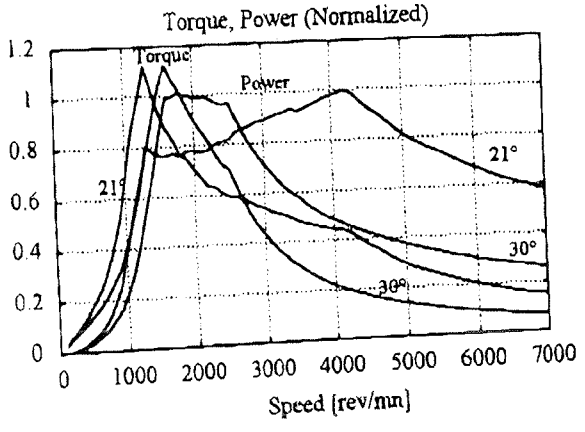

Figure 12: Torque and power characteristics for the two rotors used (FWV)

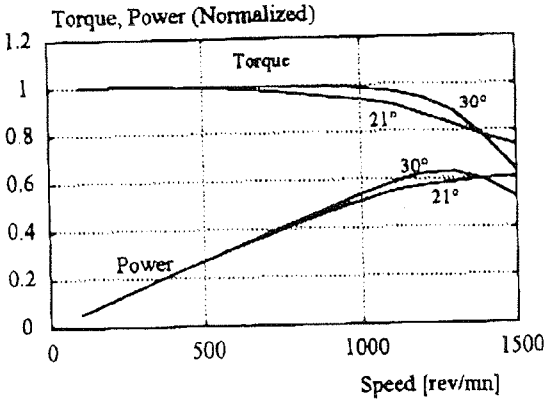

Figure 13: Torque and power characteristics for the two rotors used (TTW)

This figure, shows that for the standard rotor ($\beta_r = 21°$), base speed (ω_b) and maximal speed (ω_M) are 1300 and 4300 rev/mn respectively. For the constructed rotor ($\beta_r = 30°$), we note an increase of the base speed by about 300 rev/mn and a decrease of the maximal speed by about 1700 rev/mn. In other words the increase of β_r clearly reduces the range of operation at Constant Maximal Power.

Respectively for the two controls in torque and in voltage, we note the torque ripple between 0.5 and 0.8 for the standard rotor and 0.26 and 0.52 for the fabricated new rotor. These results show that increasing the rotor pole arc results in a net improvement of torque performances.

5. CONCLUSION

In this paper, we have studied the effect of rotor pole arc on the regime of flux-weakening of switched reluctance motor which are increasingly used in several application domains because of their simplicity and low cost. The limits of operation at maximum torque and power have been determined using real and idealized models for different structures. The present study shows that these regimes of operation are strongly sensitive to β_r and that the choice of design has to be based on a compromise between torque ripple and range of operation at constant maximal power.

6. ACKNOWLEDGEMENTS

We would like to thank all our collaborators in this work:

- LESiR (ENS de CACHAN - France),
- SACEM (Menzel Bourguiba - Tunisia),
- CETIME (Sousse - Tunisia).

7. REFERENCES

[1] B. Multon, C Glaize, "Optimisation du dimensionnement des alimentations des machines à réluctance variable", Revue de physique appliquée, N° 22, mai 1987, pp. 339-357.

[2] Données du constructeur de la tôle, "UGINE Aciers de Chatillon et Gueugnon", Juillet 1987.

[3] C. Elmas, H. Zelaya De La Parra, "A DSP Controlled switched reluctance drive system for wide range of operating speeds", IEEE Trans. On Industry Applications, 1992, Vol.27, pp. 844-850.

[4] M. Geoffroy, B. Multon, E. Hoang, R. Neji, "Couplage de méthodes pour le calcul rapide des caractéristiques électromagnétiques des machines à réluctance variable à double saillance", Colloque méthodes informatiques de la conception industrielle, ESIM Marseille, 18 juin 1993, pp. 91-90.

[5] P. J. Lawrenson, J. M. Stephenson, P. T. Blenkinsop, J. Corda, N. N. Fulton, "Variable-speed Switched Reluctance Motors", IEE Proc. B, Elect. Power Appl., Vol. 127, pp. 253-265, July 1980.

[6] J. Corda, J.M. Stephenson, "Analytical Estimation of the Minimum and Maximum Inductances of a Double-Salient Motor", IEE Proc. , Vol. 126, May 1979.

[7] B. Multon, "Principe et éléments de dimensionnement des machines à réluctance variable à double saillance autopilotées", Journées Electrotechniques Club EEA, 25-26 Mars 1993, BELFORT.

[8] J.Y.Le Chenadec, B. Multon, S. Hassine, "Current feeding of switched reluctance motor. Optimization of the current waveform to minimize the torque ripple", IMACS TC1'93, Montreal, 7-9 July 1993, pp. 267-272.

[9] J. Y. Le Chenadec, M. Geoffroy, B. Multon, "Torque ripple minimization in switched reluctance motor by optimization of current wave-forms and of the teeth shape with copper losses and V.A. silicon constraints", ICEM'94, Sept. 1994.

[10] H. Yahia, R. Dhifaoui, B. Multon, "Modélisation électromagnétique d'une machine à réluctance variable à double saillance", CMGE'95, Rades-Tunisia, pp. 120-127.